The Journal of Undergraduate Research in Physics

CONTENTS

VOLUME 5, NUMBER 1

SUMMER 1986

Published by Guilford College
for
The American Institute of Physics and The Society of Physics Students

THE JOURNAL OF UNDERGRADUATE RESEARCH IN PHYSICS

This journal is devoted to research work done by undergraduate students in physics and its related fields. It is to be a vehicle for the exchange of ideas and information by undergraduate students. Information for students wishing to submit manuscripts for possible inclusion in the Journal follows.

ELIGIBILITY

The author must have performed all work reported in the paper as an undergraduate. The subject matter of the paper is open to any area of pure or applied physics or physics related field.

SPONSORSHIP

Each paper must be sponsored by a full-time faculty member of the department in which the research was done. A letter from the sponsor to the editor must accompany the manuscript if it is to be considered for publication.

FORM

The manuscript should be typed, double spaced, on 8 1/2 x 11 inch sheets. Margins of about 1 1/2 inch should be left on the top, sides, and bottom of each page. Papers should be limited to twelve pages of text in addition to an abstract and appropriate drawings, pictures, and tables.

GENERAL STYLE

All papers must conform to the Style Manual of the American Institute of Physics. Each paper must be prefaced by an abstract that does not exceed 250 words.

ILLUSTRATIONS

Line drawings should be made with black India ink on plain white paper. If a graph is drawn on co-ordinate paper, the paper must be lined blue. Important lines should be ruled in black. Each figure or table must be on a separate sheet. Photographs must have a high gloss finish.

CAPTIONS

A brief caption should be provided for each illustration or table, but it should not be part of the figure. They should be listed together at the end of the manuscript.

EQUATIONS

Equations should appear on separate lines and may be written in black India ink.

FOOTNOTES

Footnotes should be typed double spaced and grouped together in sequence at the end of the manuscript.

SUBMISSION

Two copies of the manuscript and a letter from the sponsor should be sent to:
Dr. Rexford E. Adelberger, Editor
THE JOURNAL OF UNDERGRADUATE RESEARCH IN PHYSICS
Physics Department
Guilford College
Greensboro, NC 27410

SUBSCRIPTION INFORMATION

The Journal will be published biannually with issues appearing in Summer and Winter of each year. There will be two issues per volume.

TYPE OF SUBSCRIBER	PRICE PER VOLUME
Individual	$ 5.00
Institution	$10.00

Foreign subscribers add $2.00 for surface postage, $10.00 for air postage.

To receive a subscription, send your name, address, and check made out to The Journal of Undergraduate Research in Physics (JURP) to:

Journal of Undergraduate Research in Physics
Physics Department
Guilford College
Greensboro, NC 27410

BACK ISSUES

Back issues may be purchased by sending $10.00 per volume to the editorial office.

ISSN 0731 - 3764

The Journal of Undergraduate Research in Physics is published by Guilford College for the American Insititute of Physics and the Society of Physics Students.

VOLUME 5 1986

The Journal of Undergraduate Research in Physics

Published by Guilford College
for
The American Institute of Physics and The Society of Physics Students

ISSN 0731 - 3764

AN EDITORIAL

The professional science societies were established when the research community wanted to provide a means for communicating recent and important discoveries in the various fields. If knowledge were not communicated, the future generations would have to discover it over again. The societies provided two forums for communication; the first being talks given at meetings, a place where new ideas could be discussed and critiqued; the second, journals sponsored by the society that provided an archive of scientific discoveries. These printed records allowed knowledge to be passed on, even though the author might be long dead. The rapid growth of the body of scientific knowledge during the past century and a half was not independent of the growth of the societies.

The Society of Physics Students (SPS) has, for a number of years, sponsored meetings at which students could report on their research, discuss new ideas, and, in general, become part of the scientific community. Five years ago, the National Council of the Society of Physics Students, a body that oversees the operations of the SPS, decided to follow the lead of the other professional societies and sponsor a journal in which undergraduate students could publish the research they did during college. The decision was converted into reality by the editor of the journal and Guilford College. Now, as we begin the fifth year of publication, the National Council of the Society has made another decision that will have a profound effect on THE JOURNAL OF UNDERGRADUATE RESEARCH IN PHYSICS. Starting next year, it will be sent to all members of the society. It will truly become the journal of SPS and Sigma Pi Sigma.

As the journal moves from a readership of 700 to one of 7000, we would like to add two new sections to it. The first is a column on possible research topics for undergraduates. Many students, interested in persuing research as part of their undergraduate studies, decide not to take part in this important part of their education because they do not have ideas of topics of research that one can do with the modest equipment and resources available in many undergraduate physics departments. We know that many faculty have ideas of topics for research that can be completed by undergraduate students. The journal would be an ideal place for such ideas to be circulated in the community. If such ideas are sent to the Journal office at Guilford College, they will be published and credit given to the person sending the ideas.

The second new section will be book reviews. We have often noticed that textbooks are written for the faculty, not the students who must use them. A text will only be profitable if faculty will decide to require it for their courses. Seldom do students decide which text should be used. As a matter of fact, there is no place where a faculty member who is interested can find out student reaction to a particular text. We propose to publish post-use reviews of text books by undergraduate students. This column will give students a chance to critique the texts they used and also provide information for faculty. THIS EDITORIAL IS A CALL FOR POST-USE REVIEW OF PHYSICS TEXTS FROM THE STUDENT READERS OF THIS JOURNAL. Reviews should be submitted, along with a letter from the sponsoring faculty member, to the editorial office in the same manner as a regular article.

COMPUTER CONTROL OF A PROGRAMMABLE, MAGNETO-OPTIC SPATIAL LIGHT MODULATOR FOR REAL TIME OPTICAL INFORMATION PROCESSING

Casimer DeCusatis
Center for Electro-optics Research
Pennsylvania State University
University Park, PA 16802

ABSTRACT

In recent years the technology of optical data processing has made possible significant practical achievements in real-time information processing. Notable accomplishments have been made in the areas of white light optical signal processing and target identification by optical correlation. The development of such electro-optics systems has created a need for basic research into the applications of micro-computer control systems to optical data processing techniques. This paper examines the software for computer control of magneto-optic spatial light modulator to be used as the input plane for several systems. This modulator can be interfaced with a microcomputer to generate programmable, real-time images which may be saved on disk. We also propose the use of vector images for these applications, since they are readily rotated and scaled in real time.

INTRODUCTION

The discipline of optical data processing originated in the early 1960's when Cutrona and his associates developed its fundamental concepts (1). More recently, technological advances have made it possible to realize a wide range of practical applications in electro-optics, particularly in the area of real-time image processing. While such developments have been extremely promising, there is still a need for basic research into many fundamental aspects of optical information processing. In particular, spatial control of images in the input plane of many data processing systems must be adapted to meet the needs of real-time optical networks.

There has been a need for an electro-optical interface to address object images for the input plane of optical data processing systems. Many optical processors require an input object transparency to modulate and transmit a beam of collimated light for further optical transformations (Fourier analysis for example). Since the original input information is often not in the form of a suitable transparency, this information must be converted into an appropriate form for optical processing. While there are devices which can serve this purpose, they are limited in application by factors such as high price, excessive weight, large volume, high power requirements, poor uniformity, volatile information storage, or prolonged write and erase times (2,3). In fact, there is a lack of fast, simple methods for producing transparencies for optical data processing from input signals.

A recent technological development which should help alleviate this problem is an electrically addressed high speed two-dimensional spatial light modulator developed by Litton Data Systems (3). This device can serve as a non-volatile random access interface for optical system input. It consists of a square grid of magnetically bistable mesas (or pixels) which may be used to modulate incident polarized light by the Faraday effect. The device can be electrically switched, so that object patterns can be written on the input plane with a computer. Thus, the system could function as a programmable spatial light modulator. Since this binary-type light modulator is transparent, it is well suited for real-time object pattern generation.

It is possible to generate object images by interfacing this magneto-optic light modulator to a microcomputer system (4). The required hardware consists of a 48K Apple II with Applesoft, one disk drive, DOS 3.3, and the APPLE LIGHT-MOD interface card.

More recently this device has been used to perform joint transform correlations (8). A microcomputer based programmable optical correlator for automatic pattern recognition was also proposed (9).

THE SPATIAL LIGHT MODULATOR

The two-dimensional magneto-optic spatial light modulator (known as LIGHT-MOD, for Litton Iron Garnet H-Triggered Magneto Optic Device) can be used as the input plane of an optical image processing system. The device consists of a bismuth doped, magnetic iron garnet film which is epitaxially deposited on a transparent, nonmagnetic garnet crystal substrate. The film is then etched into a square grid of magnetically bistable mesas and current drive lines are deposited between them. The resulting device is a 48x48 matrix of mesas (see Figure 1a) and measures one-quarter of an inch square (3).

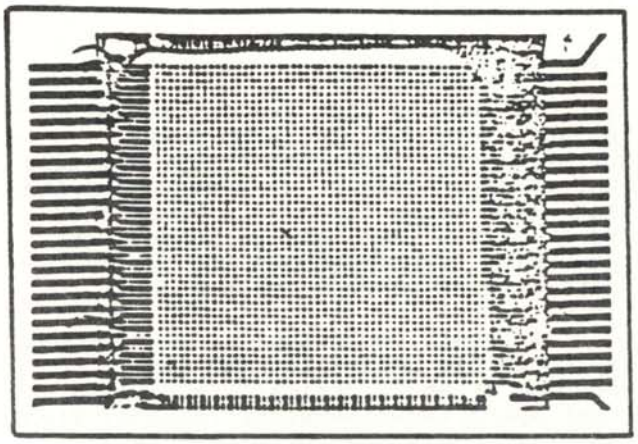

Figure 1a
Structure of the 48 x 48 LIGHT-MOD spatial light modulator (3).

When plane polarized light is incident on the device, the axis of polarization of the transmitted light will be rotated by the Faraday effect. The plane of polarization is rotated in opposite directions for opposite magnetic states (see Figure 1b). A polarization analyzer then converts this rotation into image brightness modulation. The magnetization state of the pixel may be changed by addressing current to its two adjoining drive lines. For our purposes, this switching is accomplished by microcomputer control. With an appropriate interface, it is possible to use the computer to write input patterns to the LIGHT-MOD, which in turn serves as the input for an optical image processor. This technique for generating images is well suited to a number of host systems (4,7). This work is primarily concerned with the application of such a device to a white light optical

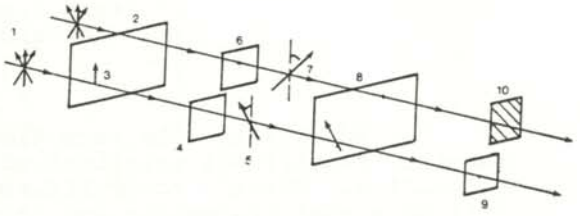

Figure 1b
Operation of LIGHT-MOD as a light valve. Unpolarized light (1) is converted to linearly polarized light by polarizer (2). Pixels magnetized in one direction rotate the plane of polarization clockwise, while those magnetized in the opposite direction rotate it counter clockwise. Analyzer (8) passes only one orientation, yielding light and dark output.

signal processor and a pattern recognition system. This paper is not concerned with the details of the interfacing circuitry, but with the problem of developing suitable software to generate and manipulate input patterns.

White Light Optical Signal Processing

The programmable, binary-type spatial light modulator has been successfully applied to optical information processing systems. When utilized in the configuration shown in Figure 2, the device is capable of

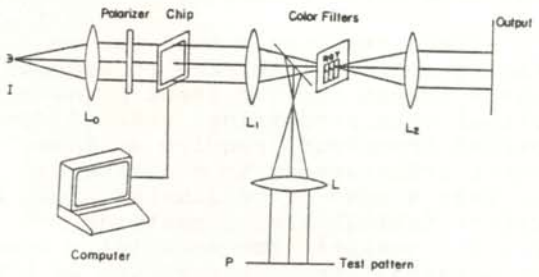

Figure 2
Host systems (4) for the spatial light modulator. White light processor using a programmable input object for pseudocolor encoding.

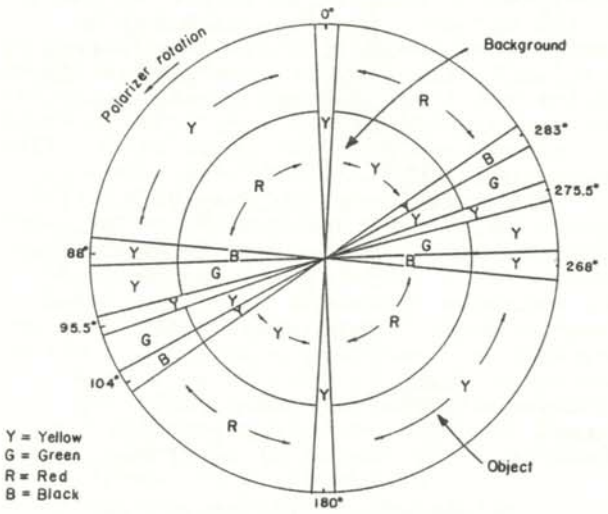

Figure 3
Color modulation as a function of polarizer angle. Transmittance characteristics of the LIGHT-MOD under polarized white light illumination (4).

generating elementary object patterns. In addition, the device responds to a wide range of colors, making it ideally suited for white light applications such as color spatial filtering.

The color of the image (magnetized pixels) and the background (demagnetized pixels) may be changed by rotating the direction of the polarization of the incident light (4). The combination of magnetized pixels and a rotated polarizer effectively acts as a wave plate for various colors. As illustrated in Figure 3, the device is capable of producing several different color combinations for varying contrast. Narrow band pass filters may also be used for color information processing.

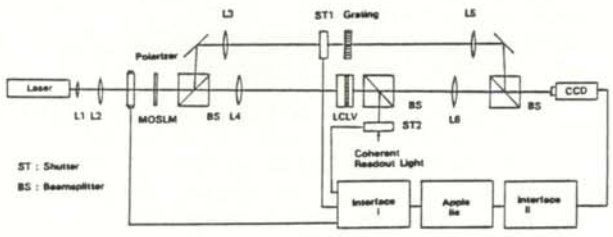

Figure 4
A microcomputer based real-time optical signal processing system for pattern recognition and image subtraction (7).

Optical Pattern Recognition

The spatial light modulator can be used as the input plane of a real-time pattern recognition system (shown in Figure 4). In order to perform pattern recognition, shutter ST2 is opened, while shutter ST1 is closed. Input patterns may be generated with the spatial light modulator when it is illuminated by a laser. The resulting optical signal passes through lens L4, which performs a Fourier transform of the input pattern. This Fourier transform falls on the front surface of a liquid crystal light valve (LCLV). The LCLV responds by producing a power spectral density on its rear surface. A coherent light is used to reflect this spectral density off the rear surface of the LCLV through more processing optics. Finally, a charge coupled device (CCD) is positioned in the output plane to transform the output intensity distribution into arrays of electronic signals for analysis.

If several input patterns are generated at the same time on the light modulator, this system can identify any two patterns which are identical. If any two input patterns to the system are identical, we will observe two autocorrelation functions diffracted about the origin of the output plane. For this application, we can neglect the grating structure of the light modulator, since it will not significantly affect the output. Thus, we may utilize the spatial light modulator as the input plane for the target identification system. By closing shutter ST2 and opening ST1, the system can perform real-tie image subtraction (7).

SOFTWARE REQUIREMENTS (10)

One of the most useful characteristics of the spatial light modulator is its ability to generate real-time images when suitably interfaced to a microcomputer allowing one to take advantage of both the speed of optical processing and the stored programs of the computer. Such a system presents difficulties in that correlation detection is generally sensitive to both the orientation and scale of the input signal. Although methods have been suggested to overcome this problem (notably the use of a scale-invarient Mellin transformation (2)), we advocate a software package capable of manipulating the input pattern in real time.

This proposed system generates high-resolution vector images which are

stored in binary files called shape tables. These vector images are unique because of the way in which they are defined by the computer. In graphics mode, it is possible to compose figures on the computer screen by issuing an appropriate command and giving the endpoints of a line segment (5). The computer will then draw the image, one line at a time. When a shape table is used, however, an entire figure is described before the computer is instructed to draw it. This description also may be saved on the disk (as a shape table) so that the computer can re-create the image at any time.

Each image in a shape table is composed of a series of bytes, from 0 to 255 ($00 to $FF in hexadecimal notation) (6). Each byte, in turn, may contain from one to three vectors. A vector describes movement in some direction (up, down, right or left on the screen). It also can tell whether or not to draw on the screen while moving.

VECTORS	BINARY CODE
Move up without plotting	000
Move right without plotting	001
Move down without plotting	010
Move left without plotting	011
Move up with plotting	100
move right with plotting	101
move down with plotting	110
move left with plotting	111

Table 1
Plotting vectors and their binary codes (6).

required for optical applications.

Images are scaled up to a maximum of 255 times the default size by lengthening each vector which composes the image . A scale of 2 implies that the image is twice as large as when its scale is equal to 1. However, the separation of individual vectors also increases proportionally. This may cause distortions at scale values greater than 20, the upper range of the practically useful image sizes. Images cannot be scaled down from the default size because this would require adjacent vectors to move closer together and plot over each other, effectively canceling each other out.

While the distortion experienced by large scale images represents an inherent property of the system, it can be easily minimized by drawing images as a continuous connection of vertical and horizontal vectors. This eliminates spaces or gaps between vectors that distort at large scales (see Figure 5). At large scales, images may partially "wrap around" the screen. To help alleviate this problem, a utility was developed to reposition images anywhere on the screen. An image thus may be manipulated until it fills the desired portion of the screen. Another utility varies the image and background color for maximum contrast.

Image rotation

The rotation of an image is controlled by the variable "ROT" which has values from 0 to 255. The default value is 0. Each integer increase in ROT causes a clockwise rotation of the image's vector components by 5.6 degrees, the smallest rotation increment which is visible on a high resolution graphics screen (5,6). A change of ROT of 1 is not readily observable for images of small scale.

Some distortion is encountered in rotations of one unit since it is the individual vectors which rotate, not the entire image. Small angle rotations, however, do not have an appreciable effect on the autocorrelation functions of the image. Distortion free rotation may, however, be accomplished in intervals of 90 degrees. The images may also "wrap around" the screen if they are positioned near one edge of the screen

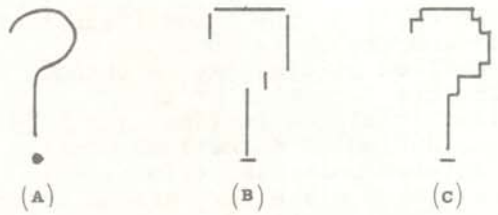

Figure 5
Sample image scaling effects. A) The original image. B)Scaled-up image when the image is defined as the intersection of line segements. C)Scaled-up image in which the original image is defined as a continuous connection of vertical and horizontal vectors.

An image is defined in the following manner. Consider drawing the image by hand on graph paper as a series of dots. Then, draw a line through each dot. The resulting outline can be represented as a series of vectors, either plotting or non-plotting. Any image can be constructed with an appropriate combination of the eight vectors listed in Table 1. By including up to three vectors in a byte, the computer makes use of 256 possible bytes to create images.

The vector zero is a special case. It means "move up without ploting" (see Table 1) only if it is the first vector in an image byte. Otherwise, this vector marks the end of an image. All images end with this termination byte.

Each image is organized into a 12-element binary file for storage on disk (6). These images then may be recalled and written to the spatial light modulator. The use of vector images rather than plotting a matrix of high-resolution points is particularly useful since the position, scale and orientation of the images can be readily controlled.

Image scaling

The relative scale of an image generated by this system is controlled by the variable "SCALE", which may be sets to the desired image size. The program permits SCALE values from 1 to 255, but we have only found use for scales from 1 to about 20 in optical processing applications. When an image is first created, it automatically assumes the default of SCALE = 1. Images only may be scaled up from this size. The scale of an image is relative. An image scale of 1 only implies that the image is currently as small as possible, not that it is similar in size to another image of the same scale. Thus an image should be created no larger than the minimum size and then rotated. As before, the images can be repositioned anywhere on the screen to prevent overlapping. The images can be rotated up to four complete revolutions from the initial position in which they were created.

System Interface

Once an image has been generated by this software package, there are several possible ways of transferring the image to the LIGHT-MOD device. For our purposes, an image (or part of an image) is first positioned on the high resolution computer screen within a 48x48 pixel square region. The screen is then scanned bit by bit. Any pixel which is "on" (bright) is then written to the corresponding position on the 48x48 LIGHT-MOD chip. The appropriate pixel on the chip is activated by means of the x-y grid of current dirve lines. The magnetic state of that pixel of the LIGHT-MOD is thus turned "on".

Using a raster scan format, each pixel on the device may be addressed sequentially by activating the appropriate pair of crossed electrod drive lines. A block diagram of the LIGHT-MOD control and drive system is shown in Figure 6. In practice, a magnetic coil is wound around the chip, which produces a magnetic field to aid in driving the chip to saturation. This is regulated by the coil driver shown in Figure 6.

The next generation of these devices is projected to be a 512x512 pixels per square. In order to control suh a device, a 16 bit microcomputer with 1 megaword addressing capability would be required (7).

Using a raster scan format, the device may be written in parallel by activating one of the horizontal electrodes and then applying a raster line signal simultaneously to the vertical electrodes. The scanning format is not limited to a conventional raster. Any desired addressing sequence may be implimented with the appropriate digital control. Various types of addressing modes are currently under development, including a multiple pixel scan format which used two or more pixels at a time (3). Each pixel on the device can be written in approximately 1 microsec. This means that a 512x512 square matrix could be addressed in .256 sec in serial mode, or in .512 msec in parallel.

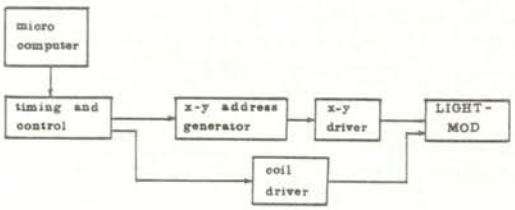

Figure 6
LIGHT-MOD control and drive system (7).

CONCLUSIONS

We have developed the software for a magneto-optic spatial light modulator controller. The resulting programmable device can be utilized as the input plane for an optical signal processing system. It is capable of storing images on disk, writing them to the light modulator, and then manipulating the images using rotations, scale changes, repositioning, and color changes to optimize the image correlation functions for optical signal processing applications. The system is useful in many real-time host systems, including white light optical signal processing and pattern recognition.

ACKNOWLEDGMENTS

The author wishes to thank Dr. F.T.S. Yu and Mr. M.F. Cao of the Pennsylvania State University's Electro-optics Laboratory for their support and guidance during this project. The inspiration of Mr. B. Kersey's "Apple Mechanic" programs are also gratefully acknowledged. All the high-resolution utilities in our work are credited to "Apple Mechanic", produced by Beagle Brothers (6).

REFERENCES

(1) L.J. Cutronaa, E.N. Leith, C.J. Palermo, and L.J. Porcello, "Optical Data Processing and Filtering Systems", IRE Transactions on Information Theory, Vol. IT-6, No 3, p. 386, (1960).

(2) F.T.S. Yu, Optical Information Processing, John Wiley, New York, (1983).

(3) W.E. Ross, D. Psaltis, and R.H. Anderson, "Two-Dimensional Magneto-Optic Spatial Light Modulator for Signal Processing", Opt. Eng., 22, p. 485, (1983).

(4) F.T.S. Yu, X. Lu, and M. Cao, "Application of a Magneto-Optic Spatial Light Modulator to White Light Optical Processing", App. Optics, 23, p.4100 (1984).

(5) W.B. Sanders, The Elementary Apple, Datamost, Inc., Reston, NY (1983).

(6) B. Kersey, Apple Mechanic (Apple Tip Book #5), published by Beagle Brothers Micro Software, (1982).

(7) F.T.S. Yu, M.F. Coa, and J.E. Ludman, "A Microcomputer Based Programmable Optical Signal Processor", Opt. Eng. (to be published), (1985).

(8) F.T.S. Yu and X.J. Lu, "A Programmable Joint Transform Correlator", Opt. Comm. 52, 10 (1984).

(9) F.T.S. Yu and J.E. Ludman, "A Microcomputer Based Programmable Optical Correlator for Automatic Pattern Recognition and Identification", Opt. Letters 11, (1986).

(10) Program listings are available from: Dr. F.T.S. Yu, Center for Electro-optics Research, Pennsylvania State University, University Park,. PA 16802

FACULTY SPONSOR OF THIS PAPER

Dr. Francis T. S. Yu, Director
Center for Electro-optics Research
Pennsylvania State University
211 EE East Building
University Park, PA 16802

THE CYRSTALLIZATION OF AN ELECTRODEPOSITED NICKEL-PHOSPHORUS ALLOY STUDIED BY X-RAY DIFFRACTION AND DIFFERENTIAL SCANNING CALORIMETRY *

Katherine A. Sanders
University of Dayton Research Institute
University of Dayton
Dayton, OH 45469

ABSTRACT

X-ray diffraction (XRD) and differential scanning calorimetry (DSC) were used to study the crystallization of a nickel-phosphorus alloy containing 23 atomic percent phosphorus. As the amorphous Ni-P sample was heated, a crystalline Ni_5P_2 phase was formed in the temperature range 270C to 315C. The activation energy for this transition was measured using XRD and a DSC kinetics program. At temperatures higher than 315C, the Ni_5P_2 phase was converted to a more stable Ni_3P crystalline state.

INTRODUCTION

An electrodeposited nickel-phosphorus alloy is amorphous; there is no long range order to the crystal lattice. Through the process of annealing, stress is relieved in the sample, and larger crystals begin to form. The process of crystallization seems to obey the Ostwald rule, which states that a system transforms from a less stable state through a series of more stable intermediate states to reach a final equilibrium state (1).

The compounds resulting from the annealing are dependent upon the phosphorus content and the amount of heating. As seen in Figure 1, a Ni-P phase diagram (2), this system is very complex. It can be seen that there are numerous phase field lines in the 20% - 30% region; the region in which the sample studied lies. The crystallization of this sample acts as if it were cooling from the melt, thus, the phase diagram is important in helping to determine various phases of crystallization.

X-ray diffraction (XRD) techniques and differential scanning calorimetry (DSC) can be used to study this crystallization. This paper is an investigation, using these two techniques, of the products resulting from the annealing of an electrodeposited nickel-phosphorus alloy in an argon atmosphere.

Background

Several studies have been done on the crystallization of Ni-P alloys using X-ray diffraction that yielded contradictory results for the temperature ranges of the transformation stages and the resulting phases. Pittermann and Ripper (3) found that during isothermal annealing

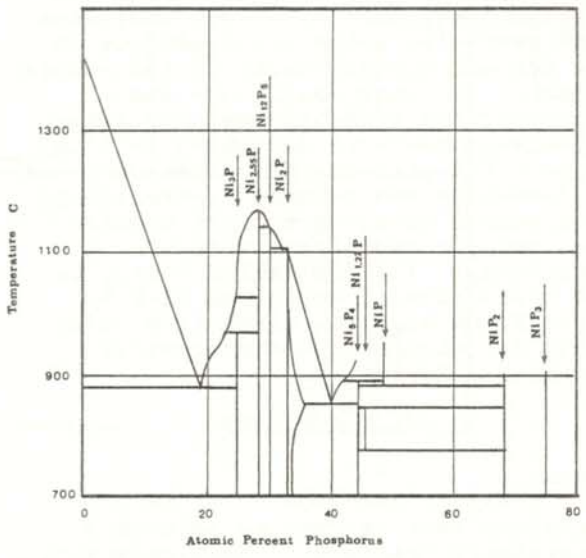

Figure 1
Phase Diagram for Ni-P. Note the numerous phase field lines in the region of 20-30% P.

of 23% P content alloys, a metastable intermediate compound Ni_5P_2 (hexagonal) or $Ni_{2.55}$ P (trigonal) occurred and the final crystallization product was Ni_3P. E. Vafaei-Makhoos (4) reported a metastable phase of Ni_5P_2 (hexagonal) and a final stable phase of Ni_3P. Clements and Cantor (5) used differential scanning calorimetry to study lower phosphorus content alloys. They found that the transformation temperatures (temperature at which the

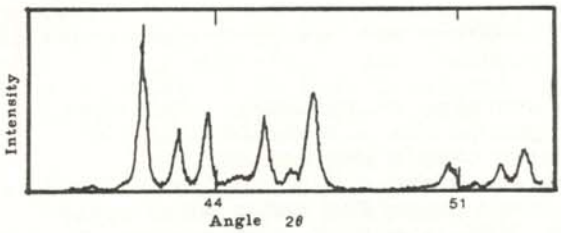

Figure 2
X-ray Diffraction Scan of crystalline Ni P. This spectrum is characterized by numerous peaks.

different crystal states occured) were dependent upon the heating rate. They found there was a 30 K drop in the transformation temperature with a change in the heating rate from 40 K/min to 10 K/min.

Previous work on electroless and electrodeposited Ni-P alloys indicated that corrosion rates are dependent on the percent crystallinity of the sample tested (7). This result and the contradictory results mentioned above stimulated the work discussed in this paper. The goal of this experiment was to determine the percent crystallinity of a sample as a function of heating time using X-ray diffraction techniques. The activation energy of the transition of amorphous Ni-P to crystalline Ni_5P_2 was determined using X-ray diffraction and differential scanning calorimetry.

THE EXPERIMENT

Theory

X-ray diffraction (XRD) is a technique that is used to determine interatomic spacings. The X-rays are incident on the sample and are diffracted by atomic layers within the crystal structure. The equation that predicts where constructive interference will occur is:

$$n\lambda = 2\,d\,\sin\theta \qquad (1)$$

where λ is the wavelength of the X-ray (Cu K α), d is the spacing between atomic layers, θ is the angle of reflection, and n is the order of the scattering.

The data are collected and graphed as intensity versus angle of scattering (twice the angle θ). A typical Ni_3P spectrum is shown in Figure 2. The angles at which constructive interference takes place (peaks in the intensity) can be determined from the data. Then, using Equation 1, the spacing between planes can be determined. Each crystalline species has a characteristic set of spacings which can be found in standard tables.

Experimental Procedure

All samples tested were taken from the same piece of electrodeposited nickel-phosphorus standard supplied by Dayton Tinker Corporation. The composition of the sample was determined by Auger Spectroscopy to be 23 atomic percent phosphorus and 77 atomic percent nickel. The samples were approximately 0.5 square inches.

The samples were heated in a Fisher model 260I tube furnace under a flow of Argon gas at 0.5 ft^3/hr. The temperature was monitored and maintained with an Omega 6100 controller in conjunction with a Keithley 195A Digital Multimeter and a Variac variable power supply. The parameters studied were temperature and heating time. After the sample was heated a specific period of time, it was allowed to cool in the argon flow. The argon flow prevents oxidation of the sample surface.

The crystalline structures of the heated samples were determined using a Norelco diffractometer with Cu Kα radiation. The X-ray diffractometer was swept through the angles 37 to 52 degrees. The X-ray diffraction apparatus was interfaced to an Apple IIe personal computer for data reduction.

The XRD data was converted to percent crystallinity using linear sensitivity factors. The relative heights of the amorphous peak and the Ni_5P_2 peak at 48.2 degrees were measured. The percent crystallinity is the ratio of the normalized Ni_5P_2 peak to the sum of the normalized peaks,

given by the relationship:

$$\% \text{ Crystallinity} = \frac{(4/12.6)C}{(4/12.6)C + A} \quad (2)$$

Where A is the Amorphous peak height, C is the crystalline peak height and (4/12.6) is the ratio of the standard amorphous height to the standard crystalline height.

Discussion

Before heating, the Ni-P samples were amorphous. Figure 3 shows an X-ray spectrum of one of them. The lack of peaks shows that there was no long range order to the crystal lattice.

The first process that was studied was the crystallization of the amorphous Ni-P into Ni_5P_2. This takes place between 270 C and 315 C. Above 315 C, Ni_5P_2 is converted to Ni_3P . The XRD pattern of this metastable phase, Ni_5P_2, corresponds only roughly to the hexagonal phase found by Pittermann and Ripper (3). Because the

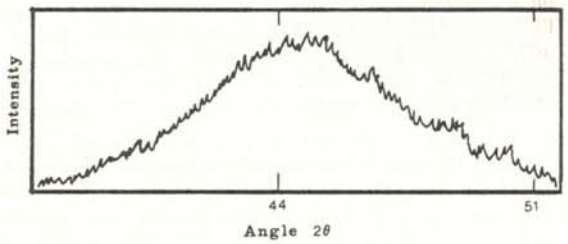

Figure 3
X-ray Diffraction Scan of Amorphous Ni-P. The spectrum is characterized by a broad peak, showning no fine structure.

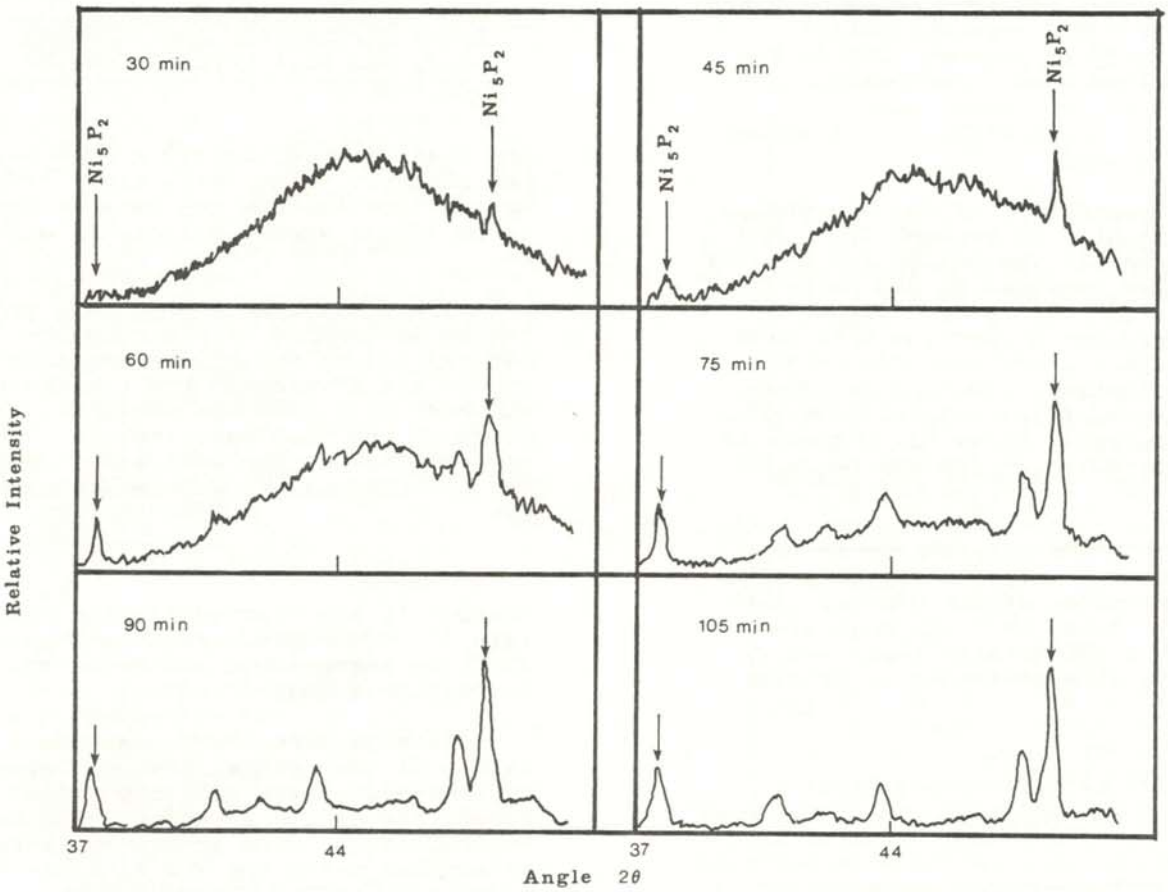

Figure 4

X-ray Diffraction Scans of Ni-P as it is heated at 270 C. As the sample is heated, the spectrum transforms from that of an amorphous medium to one that shows complete crystal structure.

samples tend to warp upon heating, it is difficult to align the sample in the diffractometer, causing a shift in the location of the peaks. Since the samples are successively heated, the problem is compounded. However, both this study and Pittermann and Ripper found d-spacings which differ from the tabulated values for Ni_5P_2 (5). The tabulated values are based on powder samples.

Figure 4 shows the results of the crystallization study done at 270 C. After 30 minutes of heating, Ni_5P_2 peaks begin to form. They can be seen superimposed on the broad amorphous peak. These peaks increase in intensity as the sample is heated. After a heating time of 120 minutes, the sample is more than 90% crystallized.

Figure 5 compares the results for crystallization at 270 C and 280 C. The rate of crystallization increases with temperature. The crystallization asymptotically approaches 100% as the length of time heated increases. Between 290 C and 315 C, the crystallization to Ni_5P_2 occurs almost instantaneously.

The temperature of the conversion of Ni_5P_2 to Ni_3P is between 320 C and 340 C. A sample was heated for 5 hours at 315 C and remained in the Ni_5P_2 phase. At 320 C, heating for 30 minutes produced a spectrum with both Ni_5P_2 and Ni_3P peaks (see Figure 6). After 15 minutes of heating at 335 C, the sample had fully crystallized into Ni_3P. Apparently below 315 C there is not enough energy to convert Ni_5P_2 to Ni_3P.

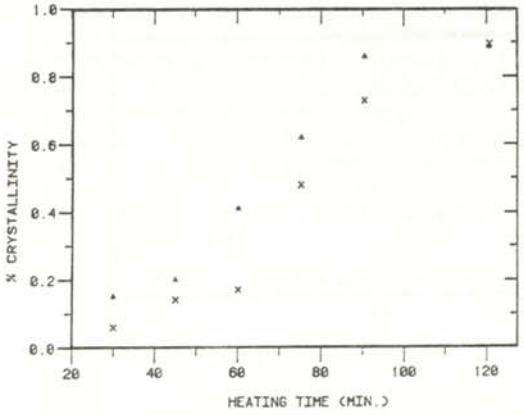

Figure 5
Percent crystallinity as a function of the heating time of a sample of NiP. The x points are done at 270 C, while the triangles are at 280 C.

The rate of crystallization can be determined from the slope of each line in Figure 5. The rate of crystallization changes with time in this process (as one can see by the change in slope of the graph). In the region 0 to 60 minutes, the rate is assumed to be linear, therefore, the rate of crystallization can be determined using the first 3 points of each line. The rate determined for 270C is 3.6×10^{-3} percent per minute,

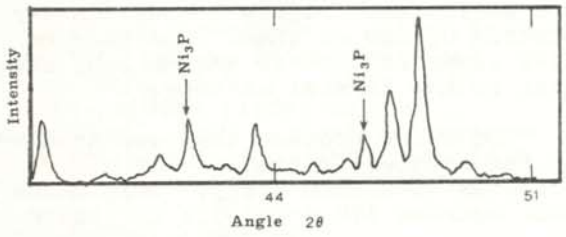

Figure 6
X-ray Diffraction Scan showing Ni_5P_2 and Ni_3P crystallization.

and that for 280C is 8.7×10^{-3} percent per minute. These rates are estimations because the rate is assumed to be linear when, in fact, it may not be.

The activation energy of a process can be determined by plotting the natural log of the crystallization rate versus the inverse of the temperature at which that rate was measured. The slope of the resultant line is proportional to the activation energy (E). The equation of this line is given by:

$$\ln k = -E/RT \qquad (3)$$

where K is the crystallization rate (min^{-1}), R the gas constant, T the absolute temperature and E the activation energy (J/mole).

In this experiment, only two values of the crystallization rate were determined. Therefore, the value determined by the equation is at best an approximation. The activation energy determined using the XRD data was 240 kJ/mole.

DIFFERENTIAL SCANNING CALORIMETRY

Background

The crystallization of the electrodeposited Ni-P alloy was also investigated using differential calorimetry (DSC). The DSC system in

this experiment was a self contained, computer interfaced system manufacured by DuPont. A sample and a reference were heated and monitored separately. They may be heated isothermally or at a specific ramp rate. The electrical energy needed to heat the samples is monitored and the differences noted. A plot of heat flow from the sample is plotted versus the sample temperature. Peaks in this plot indicate exothermic processes, which suggest the occurance of a phase change.

Results

Since the reactions in this system occur very rapidly and in a small temperature range, slow ramp rates (degrees/min) were chosen. Changing the ramp rate affects the temperature at which the exotherm (phase transition) occurs. The faster the ramp rate, the higher the temperature at which the transition occurs (see Figure 7). This

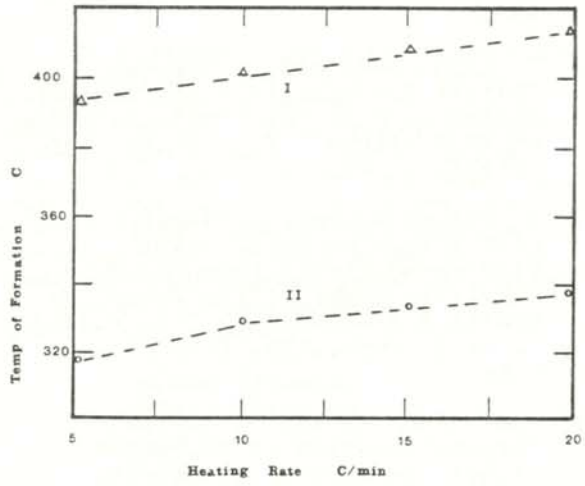

Figure 7
The temperature at which the transformation occurs as a function of the heating ramp rate. The o points are for the transition of NiP to Ni_5P_2 while the triangles are for the transition of Ni_5P_2 to Ni_3P .

agrees with the results found by Clements and Cantor (5).

Figure 8 shows the data taken at a ramp rate of 20 C/min. Two main peaks appear in the data. The first peak, labled (I), which occurs at approximately 330 C, is due to the transition of amorphous Ni-P to Ni_5P_2. The second peak (II) is due to the transition of Ni_5P_2 to Ni_3P.

There are several hypotheses for the existence of the shoulder on the high temperature side of the first transition. If the samples behave the same while heating as while cooling from a melt, the shoulder could be due to phase segregation. The phase diagram (Figure 1) shows that a 23% phosphorus sample will go through several phase fields while cooling from a melt. The 23% phosphorus line intersects the phase diagram at three points. The two transitions as well as the shoulder could correspond to the crossing of these phase field lines.

A second conjecture is that the shoulder may be due to a second form of Ni_5P_2. It is known that there are two forms of Ni_5P_2: hexagonal and trigonal. These correspond to the high and low temperature forms on the phase diagram.

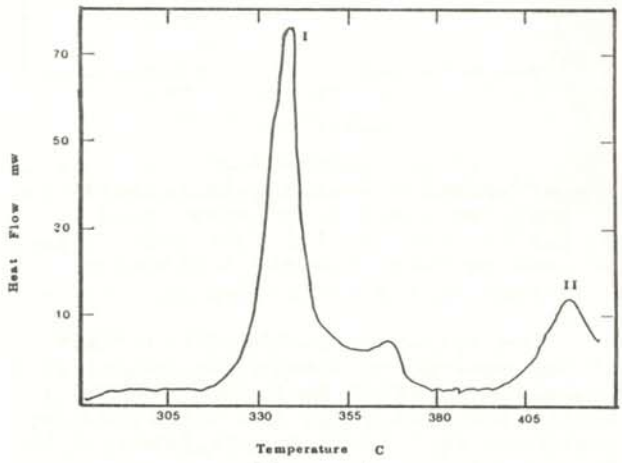

Figure 8
Differential Scanning Calorimetry Scan for a NiP film heated at 20 C/min from 270 C to 430 C. Peak I is the transition of NiP to Ni_5P_2. Peak II is the transition of Ni_5P_2 to Ni_3P .

A third possibility is that the shoulder is due to a variation in the crystallization rate due to inhomogeneous nucleation. Nucleation may be initiated on the surface due to roughness features. This is a significant consideration for these films because they are stripped from their substrates to produce a stand-alone film. The substrate side usually exhibits a higher degree of roughness than the side exposed to the bath.

Activation Energy

The Dupont system software includes a DSC kinetics program which allows one to calculate the activation energy for the phase transitions. The program uses twenty segments of the curve, corrected for changes in the heat capacity, at evenly spaced temperature intervals. The portion of the curve analyzed is that which the first segment ends at 10% of the maximum peak height and the last segment ends at 50% of the peak height.

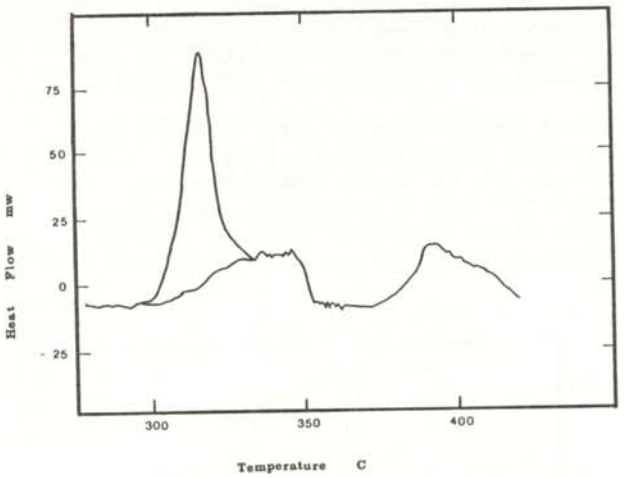

Figure 9
Differential Scanning Calorimetry Scan for a NiP film heated at 5 C/min. This is the data that were used to determine the Activation energy of the transition.

The run used for the calculation of the activation energy was ramped at 5 C/min and is shown in Figure 9. The activation energy for the transition of amorphous Ni-P to Ni_5P_2 was found to be 711 kJ/mole.

CONCLUSIONS

Two techniques were used to study the crystallization of a NiP alloy: X-ray diffraction and differential scanning calorimetry. The amorphous NiP alloy, upon being heated, forms an intermediate metastable phase determined to be Ni_5P_2 (hexagonal). Upon further heating, the sample is converted to Ni_3P. This corresponds to Ostwald's Rule and agrees with other studies.

The activation energy for the transition of the amorphous NiP to the metastable Ni_5P_2 was calculated using both methods. The activation energy found using XRD techniques was 240 kJ/mole, which is at best an approximation, and that found by DSC was 711 kJ/mole. To obtain better agreement between techniques, a better model for analyzing the XRD data must be found.

ACKNOWLEDGMENTS

The author wishes to thank Tom Wittberg, Doug Wolf, and James Hoenigman for suggesting the project and providing valuable discussions.

REFERENCES

* Present Address: Pennsylvania State University, Physics Department, 104 Davey Lab Box 84, University Park, PA 16802.

(1) The Van Nostrand Chemist's Dictionary, D. Van Nostrand Company, Inc, NY, 1953, p. 504.

(2) Adapted from: Leopold Gmelin, Gmelins Handbuch Der Anoganischen Chemie, Nickel, Teil B Lieferung 3, Verlag Chemie, GmbH., 1966, p. 947.

(3) U. Pittermann and S. Ripper, "Direct Investigation by Electron Diffraction of the Crystallization of Ni-P Alloys", Z. Metallkd, 74, (1983), p. 783.

(4) E. Vafaei-Makhoos, "Electron Diffraction Study of Newly Discovered Nickel Phosphides in Partially Crystallized Amorphous Electrodeposited Ni-P Thin Films", J. Appl. Phys., 51, (1980), p. 6366.

(5) W.G. Clements and B. Cantor, "Crystallization of Amorphous Alloys Prepared by Electroless Deposition", International Conference on Rapidly Quenched Metals, MIT Press, Cambridge, MA, (1976).

(6) Private communication: Lisa Palumbo, University of Dayton Research Institute, University of Dayton, Dayton, OH.

(7) JCPDS Powder Diffraction File, JCPDS International Centre for Diffraction Data, Swarthmore, PA , (1983).

FACULTY SPONSOR OF THIS PAPER

Dr. Thomas Wittberg
Research Institute
The University of Dayton
300 College Park
Dayton, OH 45469

AUTOMATIC DIAL-UP WEATHER SERVICE

Scott Lancaster, Varon Fugman, and Chris Eddington *
Physics Department
Principia College
Elsah, IL 62028

ABSTRACT

This paper describes a 24-hour weather service which has been provided for the students and faculty on our campus. The special feature of this 24-hour service is that the current weather data is given over the phone by a computer speaking through a speech synthesizer. Our service includes announcement of windspeed and direction, temperature, rainfall, and barometric pressure. Sensors and interfaces with an Apple II+ microcomputer are described. The synthesized weather message can be adjusted by the program. The computer detects the ringing signal, connects the phone line, and delivers the message.

INTRODUCTION

This project was started in order to provide the Principia College community with an automatic dial-up weather service. This service allows anyone interested to call a campus telephone extension and hear the weather service computer give a current weather announcement. The weather service announcement is generated by the computer based-system shown in Figure 1. The system can be divided into several subsystems:

1. Weather sensors
2. Signal processors
3. Analog to digital converters
4. Microcomputer
5. Serial output interface
6. Speech synthesizer
7 Telephone interface

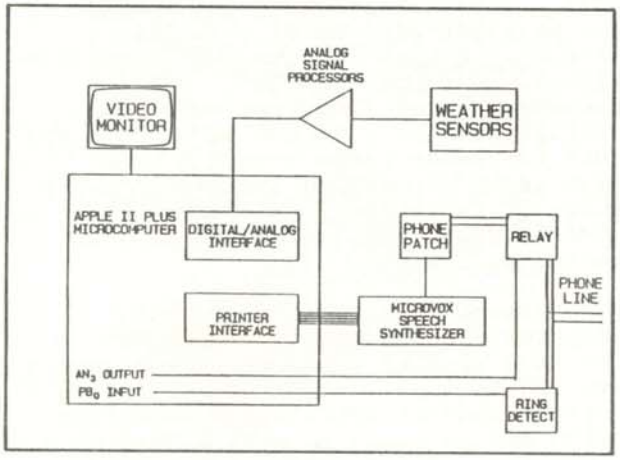

Figure 1
Block diagram of the weather service system. The ring detect, relay and phone patch comprise just one subsystem.

We will describe this system in sufficient detail that another student group could develop a system of their own.

WEATHER SENSORS

Each of the weather sensors generates an electric output voltage which varies with the weather parameter being sensed. The voltages produced by these devices vary with the device and the manufacturer. Figure 2a shows the sensors used in our system. A brief description of each follows.

Wind Speed (1) - The voltage is produced by a DC generator connected to the rotating shaft of the windvane propeller. To convert the output voltage to windspeed, one uses the relationship:

$$\text{Voltage} = .0795 * \text{windspeed (MPH)}$$

Wind Direction (1) - This voltage is a fraction of the 5.00 VDC supply placed across a 5 KOhm potentiometer whose shaft is connected to the windvane mast. The relationship between direction

and output voltage is:

$$\text{Voltage} = (5.00/360) * \text{direction}$$

Temperature (2) - This sensor behaves as a Zener diode. The Zener voltage is proportional to the absolute temperature. The voltage relationship is:

$$\text{Voltage} = .010 * \text{temperature (K)}$$

Rainfall (3) - As the rain guage fills (12 inch capacity), its mechanism turns the shaft of a 25 KOhm potentiometer. A 5.00 VDC supply is placed across this potentiometer. The device output is the fraction of this given voltage.

Barometer (4) - The sensitive element is a pressure dependent resistance in one arm of a bridge circuit.

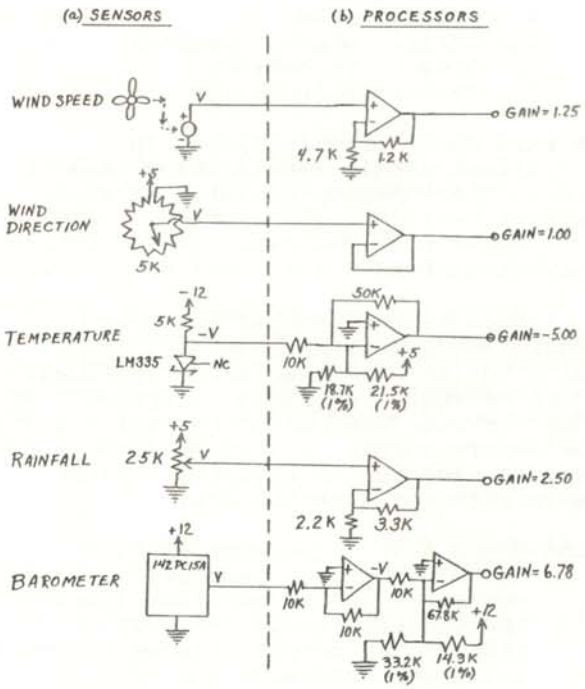

Figure 2
Schematic diagram of the weather sensor and signal processor subsystems. Sensors are described in the text and footnotes. All operational amplifiers are Type 741 and are supplied with regulated +12 VDC and -12 VDC.

The supply voltage for this sensor is 12.00 VDC. The voltage output relationship is:

$$\text{Voltage} = 1.50 + .246 * \text{Pressure (inches of Hg)}$$

The sensors should be placed according to the manufacturer's specifications. Particular care should be given in placing the wind sensor high enough to avoid effects due to ground, trees, and surrounding objects. The temperature sensor should be placed in a white vented housing of the type approved for weather service installations. The placement of the barometer is not critical.

To present the voltages from the sensors to the computer requires two steps. First, the signals must be procesed so that the voltages fall within a range expected by the digital converter system. Second, the processed signals must be converted to digital numbers for use in the computer.

SIGNAL PROCESSOR

The device which converts the signals from the analog voltages to digital numbers requires signals in the range of 0 to 5.00 volts (5). If the signal does not cover this range, the device will not utilize the full digital precision of the converter. Those of greater range will have the upper values ignored.

Our weather parameter ranges were: Wind speed 0 - 50 MPH; wind direction 0 - 360 degrees; temperature -40 to +60 C (233 - 333K); rainfall 0 - 5 inches; and pressure 28.0 to 31.0 inches of mercury. Except for the wind direction signal, none corresponds to the expected range. The rest must be multiplied and/or biased to utilize the full converter range of 0 - 5 VDC. Even if no processing is required, a stage of isolation (buffer) is advisable between the sensor and the converter.

Figure 2b shows the circuit diagrams for the signal processors for the five weather sensors. The circuits are conventional summer or multiplier applications of operational amplifiers which may be found in most electronics texts (6). All operational amplifiers are type 741 and are suppplied with, +12.0 VDC and -12.0 VDC. The signal processor subsystem was built on a circuit board and encased in an aluminum enclosure (7).

ANALOG TO DIGITAL CONVERTER

Figure 3 shows the diagram of the analog to digital converter (ADC) subsystem. It includes a 16 channel analog switch and ADC, a peripheral interface adapter (PIA) chip and a bidirectional buffer for the Apple data bus access to the PIA, and a unidirectional buffer for the Apple address bus access to the PIA (8). This subsystem was wired on an experimenter's plug-in board available from Apple Computer, INC. It was installed in slot 5 of the Apple II+ computer. Earlier work on designing data flow via a PIA port in slot 5 has been reported by Nicklin (9).

MICROCOMPUTER

The data flow is controlled by a computer program. Figure 4 diagrams the logic flow of the program. The BASIC code is available (10).

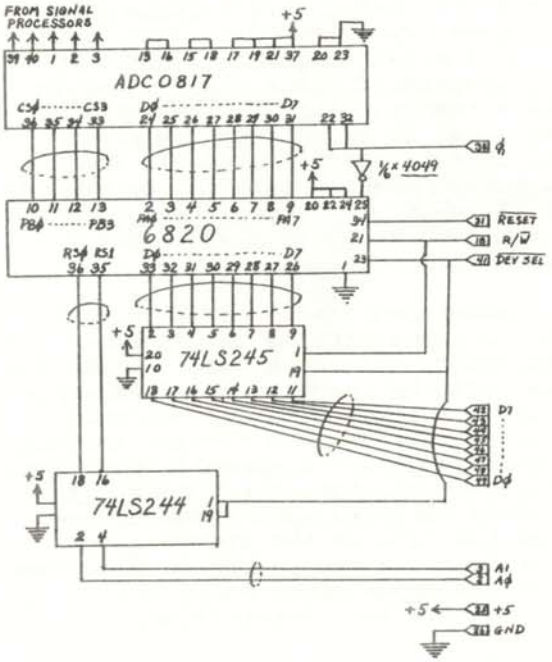

Figure 3
Schematic diagram of the analog-to-digital subsystem. Numbers and signals in the right margin refer to the Apple plug-in card pins.

The first thing the program does is initialize the variables, display the title screen, and configure the I/O ports for input and output. The program continues with the reading of the digitized data from the weather sensors. The program then checks to see if the

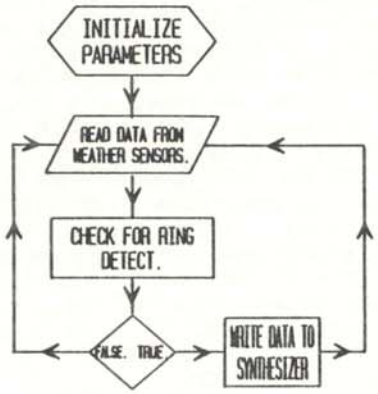

Figure 4
Flow chart of computer program for weather service.

telephone is ringing. If not, it goes back to reading and updating the weather data. However, if the telephone is ringing, the computer answers it using a phone interface circuit (see Figure 5). The current weather data is then written to the speech synthesizer. When this is completed, the computer hangs up and goes back to reading the weather data and checking the ring detector.

SERIAL INTERFACE

Weather data must be sent by the Apple II+ through a data port to the speech synthesizer. The synthesizer appears to the computer as if it were a printer. The output interface may be either a serial or a parallel device. While a parallel interface should be simpler in principle, we did not succeed in making a parallel interface work. The cause of our failure was not determined.

We therefore chose a serial interface which ran at 300 BAUD, used a 7-bit word with no parity check. The system worked immediately. So, our choice of interface type was based on convenience. Selection of the serial card is not critical. We have used two different versions successfully (11).

SPEECH SYNTHESIZER

The computer communicates verbally with a caller over the telephone lines by sending text characters to a Microvox speech synthesizer (12). The computer is connected to the synthesizer by the serial interface described above. When the synthesizer receives characters or groups of characters in a stream of text, it compares them with stored sounds called phonemes. The phonemes are stored in read-only-memory (ROM) within the synthesizer. They represent the finite set of sounds that the device can pronounce in response to combinations of characters. After the synthesizer decides which phonemes compare most favorably with the text, the audio frequency sounds are fed to the output of the synthesizer.

TELEPHONE INTERFACE

The problem to solve now is how the synthesizer can talk over the

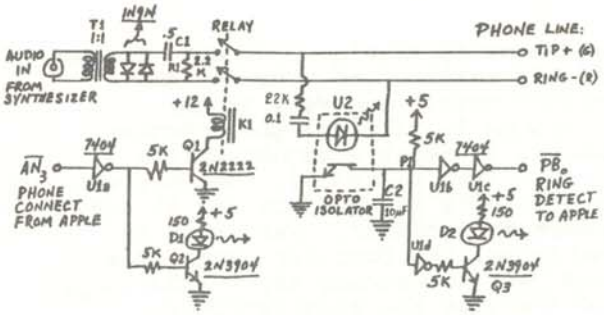

Figure 5
Schematic diagram of the telephone interface subsystem. This includes the ring detect, the connect relay, and the phone patch.

telephone. In addition to speaking the weather message, the computer must be able to determine when the telephone rings, answer when it does, and hang up when it is finished. Our custom-built telephone interface does these tasks. This interface consists of a ring detector, a relay for connection to the telephone line, and a phone patch circuit. These are built into one unit hooked to the telephone line, computer and speech synthesizer. Figure 5 shows the circuit diagram of the interface. While telephone patches are common, our design was created specifically for the Apple II computer. Consequently, we will detail the electronic principles of the phone patch.

When the telephone rings, a 90-volt AC signal appears across the telephone line. This voltage turns on the LED in the opto-isolator U2 which causes a number of things to happen. The capacitor C2 (charged to 5 Volts) is discharged by the current drain through U2. The point P1, which was at logic HIGH before capacitor C2 discharged, becomes logic LOW. The voltage inverter (U1d) changes the LOW to a HIGH, which turns on transistor Q3. Current now flows through Q3, turning on LED D2, which is the RING DETECT light. Inverters U1b and U1c provide a "clean" logic LOW at computer input port B0. Thus, the computer knows that the telephone is ringing.

Once the computer knows that the telephone is ringing, it must make the telephone connection. This is similar to lifting the receiver off the hook. The computer does this by forcing the output port AN3 LOW. The voltage inverter U1a makes this a logic HIGH, turning on transistor Q2. This turns on LED D1, the TALK light. At the same time, transistor Q1 is also turned on which actuates relay K1. Resistor R1 draws about 20 ma DC from the phone line. This is sufficient drain for the telephone company's computer to know that the phone is now "off the hook". In other words, the computer just answered the phone.

Transformer T1 serves as a match from the phone line to the speech synthesizer. Diodes D3 and D4 keep the audio from the speech synthesizer from getting too loud. The capacitor C1 blocks DC current from flowing through the transformer, which would otherwise seem like a DC short-circuit to the telephone company. The computer now writes the data to the speech synthesizer and the person on the other end of the phone lines hears the up-to-date weather information.

After the data are written, really spoken by the synthesizer, the computer hangs up the phone by forcing AN3 HIGH. This turns off transistor Q1 which releases relay K1, causing the telephone company's computer to think that the line has "hung up". The computer then goes back to reading weather data and waiting for another caller.

ACKNOWLEDGMENTS

Many persons have contributed to the work. E. Andersen built the first sensor and signal processor. K. Bol built the first computer controller and was assisted by C. Herrington, C. Wanjiru, and W. Greene in writing various computer programs. S. Struthers and T. Clayton helped select the Apple computer and designed early display models. We are also grateful to Professors T. Holzberlein and F. Marshall for invaluable advice and assistance with concepts and instrumentation.

REFERENCES

* This project was supported in part by an Allied-Bendix Research Grant administered by the Society of Physics Students.

(1) Wind speed and direction sensor: Type 102 Windvane, Weathermeasure Weathertronics, Division of Qualimetrics, INC., PO Box 41039, Sacramento, CA 95841.

(2) Temperature sensor: Type LM335 integrated circuit, National Semiconductor, INC.

(2) Rainfall sensor: Type 551 rain guage, Science Associates, INC, Box 230, 230 Nassau Street, Princeton, NJ 08540.

(4) Barometer: Type 142PC15 integrated circuit, Microswitch, Division of Honeywell, INC., 11 West Spring Street, Freeport, IL 6103.

(5) The range of signals accepted depends upon the converter chip used and the supply voltage. The range 0 to 5.00 VDC is common to many converters.

(6) See, for example, Horowitz and Hill, The Art of Electronics, Cambridge University Press, New York, 1980.

(7) Radio Shack Catalog number 270-274.

(8) While direct (unbuffered) connection to the data and address busses is simpler, it could result in timing errors owing to overload of the busses. Apple Computer, INC., recommends buffering. We did not try the system without a buffer.

(9) R.C. Nicklin, Computers and Electronics, August 1983, p.63.

(10) For a listing of the program write to: Professor D. Cornell, Physics Department, Principia College, Elsah, Il 62028 618-374-2131.

(11) Super Serial Card, Apple Computer, INC., and RS232 Card for Apple II, XICOM Computer Products, INC., 1510 Montgomery Road, Longwood, IL 32750.

(12) Steve Ciarcia, "Build the Microvox Text-to-Speech Synthesizer, BYTE, Sept. 1982, P. 64.

FACULTY SPONSOR OF THIS PAPER

Professor David A. Cornell
Physics Department
Principia College
Elsah, IL 62028

A STUDY OF THE RADIOACTIVE FALLOUT FROM THE CHERNOBYL REACTOR ACCIDENT

Mary Jayne Adriaans and Gerard M. Dion
Department of Physics
University of California, Irvine
Irvine, CA 92717

ABSTRACT

For three weeks following the reports of the Chernobyl nuclear reactor accident of April 26, 1986, particulate matter was filtered from the air near the University of California, Irvine Physical Sciences building. Gamma ray energy spectra were constructed by analyzing the filters in a sodium-iodide photon detector. The natural background activity was reduced, using a cosmic ray veto counter and a lead house, to a level that allowed us to see an increase in radiation levels over samples taken prior to the arrival of the "fall-out" cloud. The radiation increase was attributed to the nuclear reactor accident in the Soviet Union. The fission products identified were ^{103}Ru, ^{131}I, ^{134}Cs and ^{137}Cs. The half life of the gamma ray peak near 365 keV was determined to be 8.6 ± 6 days, identifying it as ^{131}I. A lower limit of the activity present in the air for ^{131}I was measured to be 12 ± 2 pCi/m^3. This is approximately a 40-fold increase over the least detectable activity over background for the iodine region of our spectra.

INTRODUCTION

On April 28, 1986, increased levels of radiation were detected in Sweden. Later reports indicated that the radiation was being emitted from a nuclear reactor accident in the Soviet Union. News agencies in the United States offered conflicting reports whether or not increased levels of radioactivity could be detected in the California area when the radiation cloud reached the state. We decided to undertake the task of detecting the radioactive fallout by filtering the air and identifying any radioactive fission products we collected in the filter.

EXPERIMENTAL PROCEDURE

In this experiment we detected increases in radiation present in particulate matter filtered out from the air. We placed coffee filters over a funnel which was covered with plastic mesh. The air was forced through the funnel by a heavy duty shop vacuum cleaner. We chose ordinary coffee filters as they did not impede the air flow as much as normal laboratory filters. The apparatus was placed at ground level behind the Physical Sciences Annex building at the University of California, Irvine.

We pulled air though the filters for one hour intervals and collected nine samples over a three week period. The particulate matter in the filters was analyzed using a sodium-iodide gamma ray detector, surrounded by a lead house to reduce the background counting rate and covered by a cosmic ray veto counter to greatly reduce counts from cosmic rays. Within a few days of the collection of particulate matter, each filter was placed in the detector for twelve hours. After each gamma ray spectrum was completed, we stored the spectral data on magnetic tape for later analysis.

A list of possible fission fragments that might occur in a reactor accident was generated. The gamma ray energies of these fission fragments were determined (see Table 1). We checked the spectra collected from the various filters for increases in number of gammas at these energy ranges. The results are shown in Table 2.

ANALYSIS AND RESULTS

Identification of Background

The background radiation for this experiment was defined by the filter samples that were collected before the arrival of the fallout cloud. Spectra collected for such cases are shown in

Figure 1. We chose samples #3 and #4, collected on 5-5-86 and 5-7-86 respectively, as background levels. We were unable to identify any specific peaks in our samples due to background activity because of the 30 to 60 Kev energy resolution of our detector. When the background samples were checked with a Ge(Li) detector, with energy resolution of 5 keV, we could identify background airborne isotopes including ^{214}Bi (radon series) and ^{208}Tl (thorium series) and ^{40}K.

Isotope	Half-life	E (keV)	Intensity
^{103}Ru	40 days	497	.90
^{131}I	8.05 days	364.5	.82
^{134}Cs	2 years	604.7 795.8	.98 .88
^{137}Cs	30 years	661.6	.85
e^+, e^- *	-	511	-

* (Annihilation Radiation)

Table 1
Summary of isotope information. These are the isotopes of the fission products indentified in sample #6. The intensity is expressed as the number of gamma rays emitted per decay of the parent isotope.

Identification of Fission Products

Sample #6, whose spectrum is shown in Figure 2, taken on 5-12-86 displayed surprising differences from the background values. This sample was analyzed in the Ge(Li) detector so that we could accurately identify the isotopes present in our sample. The results of this analysis revealed a significant increase over background in the isotopes ^{103}Ru, ^{131}I, ^{134}Cs and ^{137}Cs. These are known to be fission products. Samples #7 - #9, shown in Figure 4, continued to show higher levels of radiation than the background samples, but they were not as prominent as the levels in sample #6.

Sample Number	Date Collected (time of day)	Date Analyzed	Total counts (all energy)	Number of counts within energy range of fission products (Energy range keV)			
				^{131}I 320-434	^{103}Ru 454-593	^{134}Cs ^{137}Cs 590-763	^{134}Cs 760-905
3	5/5/86 (20:25-22:27)	5/8/86	36,899	3,959	3,566	3,085	1,938
4	5/7/86 (10:00-12:30)	5/10/86	40,028	4,350	3,940	3,291	2,103
5	5/9/86 (12:50-13:50)	5/13/86	40,842	4,536	4,109	3,437	2,097
				peak 2	peak 3	peak 4	peak 5
6a	5/12/86 (12:10 - 13:20)	5/15/86	122,136	20,511	15,529	15,054	5,938
6b	5/12/86	5/19/86	102,756	15,971	13,746	13,159	5,214
7	5/16/86 (16:00 - 17:00)	5/18/86	56,289	7,039	6,784	5,742	2,887
8	5/19/86 (11:00 - 12:00)	5/20/86	52,751	6,417	6,136	5,174	2,561
9	5/23/86 (13:30 - 14:30	5/25/86	50,601	5,934	5,949	4,695	2,458

Table 2
Summary of data for the seven samples analyzed. All samples were analyzed for twelve hours. The counts were collected for this period of time.

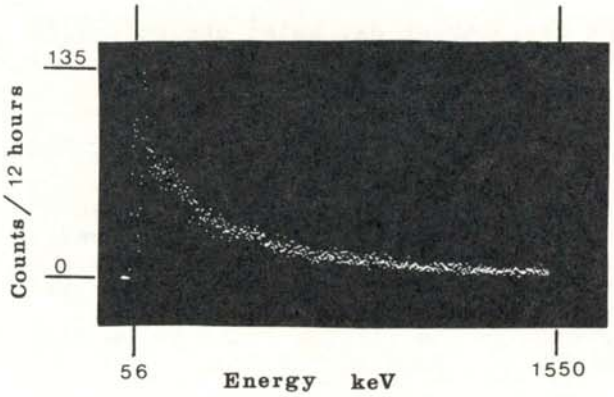

Figure 1
Typical background sample (samples #3, #4 and #5) collected May 5 through May 9, 1986.

The date on which sample #6 was taken corresponds to the day that news reports announced the arrival of the cloud over Southern California. This date was also in close correspondence with the date of the strongest radiation levels reported by the reactor facility at the University of California, Irvine.

Sample #6 was run through the NaI analyzer a second time on 5-19-86, four days after the first analysis (see Figure 3). There was a general decrease in the radiation level of about 23% and a decrease of approximately 27% in the ^{131}I peak. Using this data, we were able to experimentally measure the half life of the ^{131}I peak using the following relationships:

$$N(t) = N(0)\ \exp(-\lambda t) \qquad (1)$$

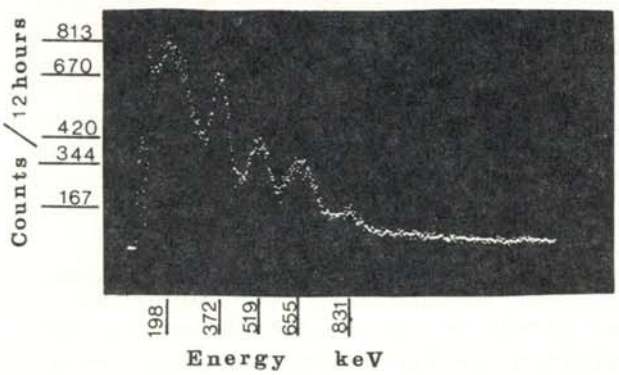

Figure 2
The first active sample (#6a) collected May 12, 1986.

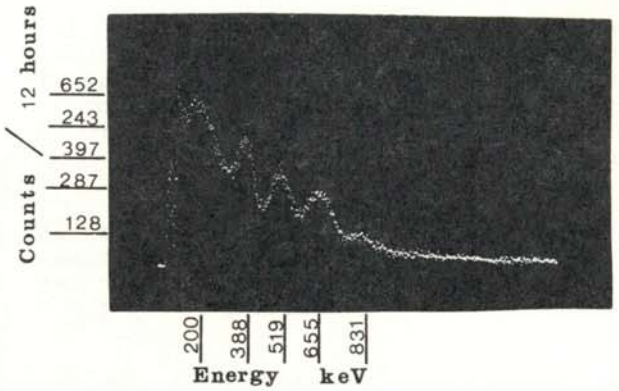

Figure 3
Re-analysis of the first active sample 4 days after the analysis done for Figure 2. This was used to determine half-lives of the fission products detected.

and

$$T = \ln 2 / \lambda \qquad (2)$$

where T is the half life of the decay and N is the number of counts, minus background in the photopeak. So, using the data for day 0 (sample 6a) and day 4 (sample 6b), one gets:

$$\lambda = -\ 1/4\ \ln\left[\ N(4) - N(0)\ \right] \qquad (3)$$

which results in a half life of 8.6 ± .6 days. The accepted value for the half life of ^{131}I is 8.05 days. This result supports our assumption that peak #2 in sample #6 is mostly, if not soley, due to ^{131}I.

The ^{131}I data were used to set a lower limit on the amount of iodine present in the air on 5-12-86. The net efficiency (NE) of the NaI detector for 365 keV gamma rays was determined to be 20±2% (1). Microscopic examination of the coffee filter indicated that particles greater than 35 microns in size had a high probability of being captured. The air flow rate (AFR) of the vacuum cleaner was measured to be .091 ± .007 m^3/min. The activity of ^{131}I present in the air could be determined using the following relationship:

$$\text{source strength} = N*C/(NE*I*CT*AFR*AT) \qquad (4)$$

where N is the number of counts, I is the intensity of the gamma ray, CT is the collection time, AT is the analysis time and C is the conversion factor from counts/sec to Curies (3.7×10^{10} counts/sec/Ci).

The value calculated in this manner would be the source strength at the beginning of the measurement time. This can be corrected for the four day delay between the collection day and the measurement day using the following relationship:

$$S(0) = S(4)*\exp(4\ln 2/T) \qquad (5)$$

where S(0) is the original source strength, S(4) is the strength after 4 days and T is the half life (in days) of the decay. Using corrected data and assuming a 100% capture efficiency, the lower limit on the activity of ^{131}I present in the air was found to be 12±2 pCi/m^3.

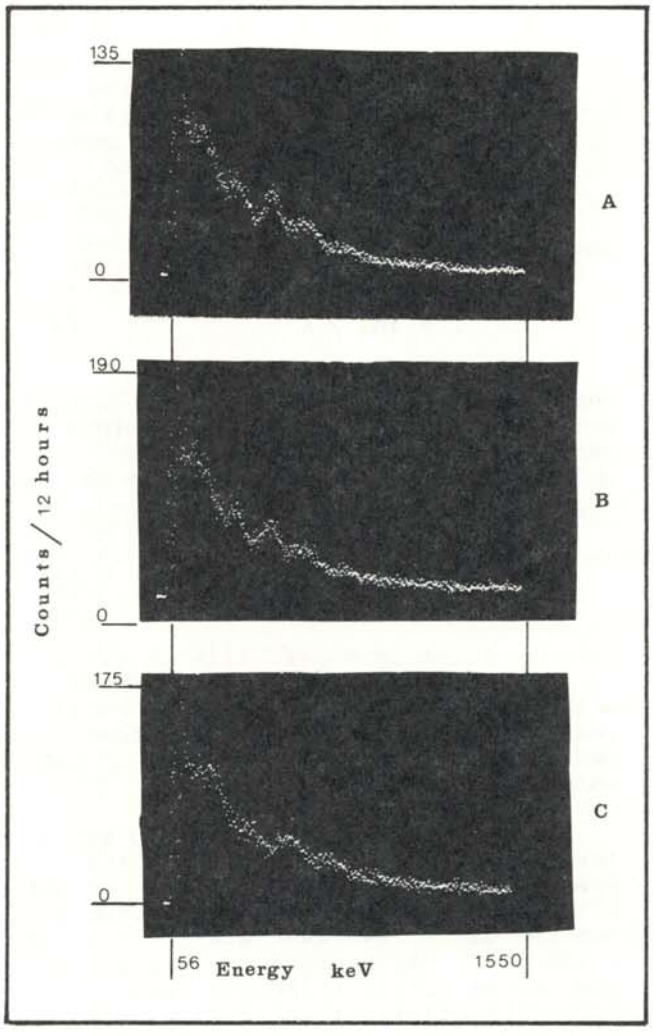

Figure 4
Samples collected after May 12, 1986. They show smaller amounts of fission products in the particulate matter collected in the filter. The data in Figure 4a were collected on May 16, Figure 4b on May 19, and Figure 4c on May 23, 1986.

The lower limit of the detectable level of activity for ^{131}I using our detector was determined by a Monte Carlo study to be .3 pCi/m^3. We simulated the background with a straight line function of energy of negative slope. The iodine decay was simulated as a Gaussian distribution. Fluctuations of the background and signal were simulated using a random number generator. We continued adding counts in this manner until a detectable peak appeared above the background activity. This occurred at an equivalent activity of .3 pCi/m^3. The measured peak was an increase of a factor of 40 over this minimum detectable level of ^{131}I.

IMPROVEMENTS

If we had know beforehand that we would detect the increase in radiation levels due to the Chernobyl accident, there are a few things that we would have d one differently. The initial rise that was recorded in our detector on the 12th of May was not analyzed until the 15th of May. Any isotopes with a short decay time and low activity level (near our detection threshold) would have dropped below detectable levels as these four days passed. We cannot be sure how many, if any, isotopes were not seen by waiting these four days. We would also have taken filter samples each day so that we could have had a more continuous sample of data, giving a better idea of when the increased levels of radiation were first detectable.

CONCLUSIONS

The detection of the four fission products in sample #6 over sample #3 and sample #4 can be attributed to the radiation released into the atmosphere by the damaged core of the Chernobyl reactor. We assumed that the increase

in the number of counts observed in our analysis is proportional to the increased levels of radiation present in particulate matter in the air. Our lower limit value for the activity of ^{131}I, 12±2 pCi/m^3, is well below the maximum permissible concentration in air (2). The federal regulations allow 100 pCi/m^3 of soluble radioactive ^{131}I and 10,000 pCi/m^3 of insoluble radioactive ^{131}I.

ACKNOWLEDGMENTS

The authors would like to thank Dr. Alan A. Hahn for his support and guidance through this study, and Dr. M. Moe for his useful suggestions regarding the filtering of air to capture particles. We are most appreciative of Donna S. Womble who spent a great deal of time helping acquire data for this project. The authors would also like to express their appreciation to the members of Double Beta Decay, the Neutrino Group and the staff of the University of California, Irvine reactor facility for use of equipment and for their support and encouragement.

REFERENCES

(1) Harshaw Radiation Detectors, Part I, pp. 9-10.

(2) Code of Federal Regulations, Title 10, Part 20, Appendix B.

FACULTY SPONSOR OF THIS PAPER

Professor Alan A. Hahn
Department of Physics
University of California, Irvine
Irvine, CA 92717